Progress In Electromagnetics Research C, Vol. 123, 91–99, 2022

Four-Element Compact and Dual-Band MIMO Antenna with Self-Decoupled Mechanism for 5G Applications

Achari P. Abhilash[1, *], Paulbert Thomas[2], Karamkulambel K. Indhu[1], Kinatingal Neema[1], Ramakrishnan Anil Kumar[1], and Chandroth K. Aanandan[3]

Abstract—This paper describes the concept and implementation of a compact dual-band microstrip slot antenna and its four-unit multiple-input–multiple-output (MIMO) implementation for sub-6 GHz utilizations. The proposed structure comprises a 50 ohm microstrip monopole on the top side with a defective ground structure (DGS) having semicircular and rectangular slots. This quad-element MIMO antenna has a size of $60 \times 60 \times 1.6\,\text{mm}^3$. The proposed antenna provides wide impedance bandwidths of 23.7% (2.42 GHz to 3.07 GHz) for the first band and 42.2% (4.14 GHz to 6.37 GHz) for the second band with a mutual coupling value less than −34 dB for the two bands. The antenna also provides a low envelope correlation coefficient, good antenna gain, and acceptable radiation efficiency across the frequency ranges.

1. INTRODUCTION

The future of wireless communication should require a high-quality, fast method for transmitting information, as well as smaller device dimensions, making MIMO antenna technology more desirable with respect to capability unless the usage of extra spectrum or radiation power [1]. Furthermore, technological advancements in contemporary wireless technology have resulted in enhanced spectrum appropriation. MIMO antennas are now widely used to increase spectrum efficiency. Antennas that cover a wide frequency range having better separation to individual antenna units are involved here.

MIMO antennas are used for a variety of purposes, including improving isolation and increasing bandwidth. In any shared substrate MIMO system, compactness and adequate isolation between radiating parts are major challenges. A polarization diversity array antenna for WLAN, WiMAX, and LTE utilizations with a dimension of 70 mm × 70 mm and a minimum isolation of 17 dB is explained in [2]. A quad-module antenna arrangement for WLAN applications with measure of 80 mm × 60 mm with 25 dB isolation is introduced in [3, 4]. A proximity coupled feeding mechanism and rectangular slits for 2.4 GHz applications are used here. The isolation level is better than 25 dB, having an overall antenna dimension of 60 mm × 80 mm in [4]. In [5], a 2 × 2 antenna system of size 67 mm × 67 mm for WLAN applications for 2.4/5.2/5.8 GHz is presented with isolation of 24 dB. An eight-port dual-band slot antenna with a T-shaped slot and an inverted U-shape feed line for common-mode suppression with a gross antenna dimension of 62 mm × 62 mm is presented in [6]. A wideband four-port MIMO antenna with a microstrip feedline with a shared ring-shaped ground plane and radiating element is introduced for 2.4 GHz Wi-Fi and 2.6 LTE application with a comprehensive antenna dimension of 120 mm × 140 mm [7]. A dual-port planar inverted F antenna with inverted L and J shaped slots acquiring overall dimension of 100 mm × 50 mm and isolation more than 15 dB is presented in [8]. In [9], a four-port MIMO antenna for 2.45 and 5.2 GHz mobile communication is introduced with a size of 50 mm × 100 mm.

Received 5 July 2022, Accepted 17 August 2022, Scheduled 24 August 2022

* Corresponding author: Achari Parambil Abhilash (abhilashap@cusat.ac.in).

[1] Department of Electronics, Cochin University of Science & Technology, Kerala, India. [2] Department of Electronics, The Cochin College, Kerala, India. [3] ACARR, Cochin University of Science & Technology, Kerala, India.

A miniaturized four-element MIMO antenna having a metamaterial dependent slow wave framework for antenna size reduction, and mutual coupling reduction is explained in [10]. A broadband-quad-module MIMO antenna configured for 5G utilities employing an 'EL' modeled slot within the radiating element is explained in [11]. A two-element split-ring resonator loaded antenna without decoupling mechanism is highlighted in [12]. A four-element MIMO antenna consisting of dual-elliptically tapered antennae modules laid out in orthogonal fashion provides large antenna size of 66 mm × 66 mm which is highlighted in [13]. The isolation enhancement using multilayer antenna design which consists of a four-port double-side printed MIMO antenna incorporated with electromagnetic bandgap structures for isolation enhancement is explained in [14], and the bandwidth and gain of the MIMO antennas are improved by high impedance surface loadings such as artificial magnetic conductor metasurface [15], bandwidth and isolation enhancement using Mu and epsilon zero based metamaterial superstrate with large antenna size of 105 mm × 72 mm [16], and isolation improvement using a metamaterial based superstrate with a large antenna volume of 180 mm × 90 mm × 27 mm [17]. In [18], the authors use a reversed arrangement of CRLH unit cell antennas to create a compact 2 elements MIMO antenna with the strong isolation of 35 dB.

A quad-ported MIMO antenna having dual-band functioning suited for sub-6 GHz operation is reported in this paper. DGS is employed for antenna size reduction, and a self-decoupling technique is used to enhance antenna isolation by positioning antenna constituents in an orthogonal configuration. The suggested antenna has compact antenna size, wide impedance bandwidth (IBW), good radiation performance, high efficiency, and reasonable gain for impending sub-6 GHz 5G implementations.

2. ANTENNA GEOMETRY AND DESIGN

Figures 1(a) and 1(b) show the schematic arrangement of the proposed single element dual-band antenna. The suggested antenna is fabricated on an FR-4 substrate with dimensions of 25 mm × 25 mm × 1.6 mm, relative permittivity of 4.4, and loss tangent of 0.02. The antenna structure contains a 50 Ω microstrip line of length $L_f = 15$ mm and width $W_f = 3$ mm with a partial ground plane on the back side. The input reflection coefficient (S_{11}) of the proposed dual-band single antenna is illustrated in Fig. 2. The antenna design starts by inserting a rectangular slot of width $W_g = 25$ mm and length $L_g = 15$ mm in the ground plane, which leads to the first resonant frequency centred 2.6 GHz as depicted as case-I in Fig. 2. Further, a semicircular slot of radius $R_g = 4.5$ mm is inserted in ground plane which ushers to the second band having wider bandwidth depicted as case-II in Fig. 2. The complete antenna structure is simulated using CST Microwave studio. The optimized parameters are $L = 25$ mm, $L_g = 15$ mm, $L_f = 15$ mm, $W = 26$ mm, $W_g = 25$ mm, $W_f = 3$ mm, and $R_g = 4.5$ mm.

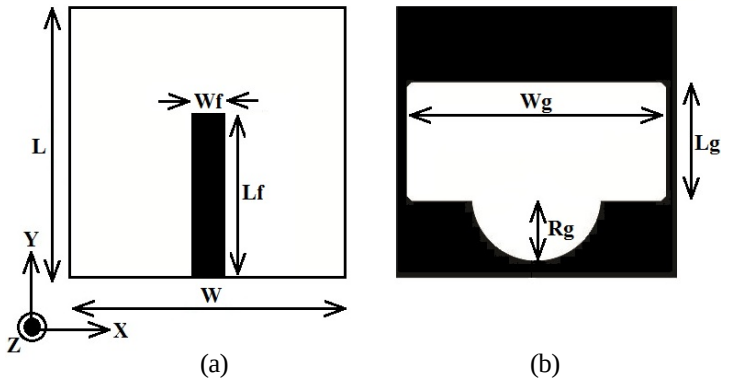

Figure 1. Schematic view of proposed single antenna unit. (a) Top view. (b) Bottom view.

The surface current distributions for the antenna at two resonant frequencies are shown in Fig. 3. In Fig. 3(a), most of the surface currents are concentrated near the left and right side edges, and the current path is identical to a quarter wavelength at the first resonance 2.6 GHz ($\lambda/4 \cong c/4f\sqrt{\varepsilon_{eff}}$,

where ε_{eff} is the effective relative permittivity of the substrate used) [6]. Fig. 3(b) depicts the current distribution at 5.8 GHz, where more surface currents are focused near the semicircular slot.

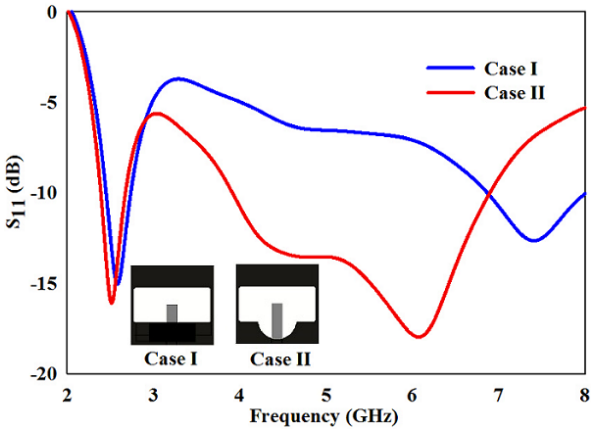

Figure 2. Input reflection coefficient (S_{11}) response corresponds to design stage-1 and design stage-2 for the proposed single element antenna.

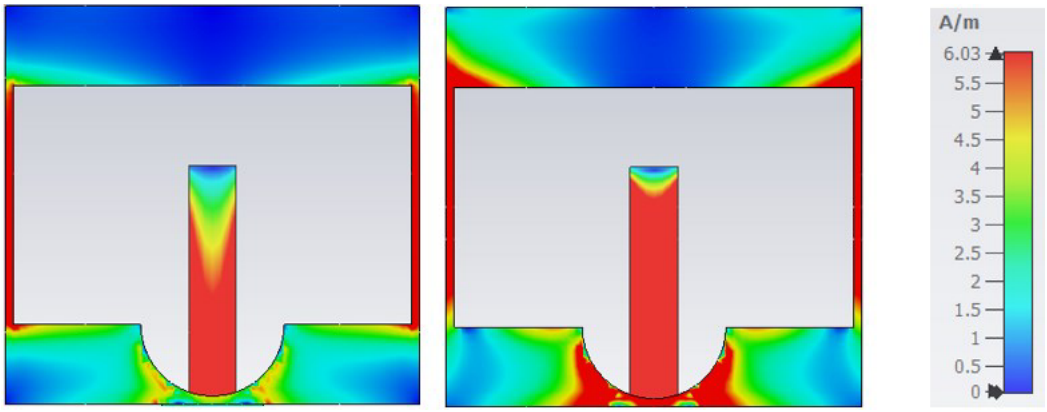

Figure 3. Simulated surface current distributions of the proposed antenna for (a) 2.6 GHz, and (b) 5.8 GHz.

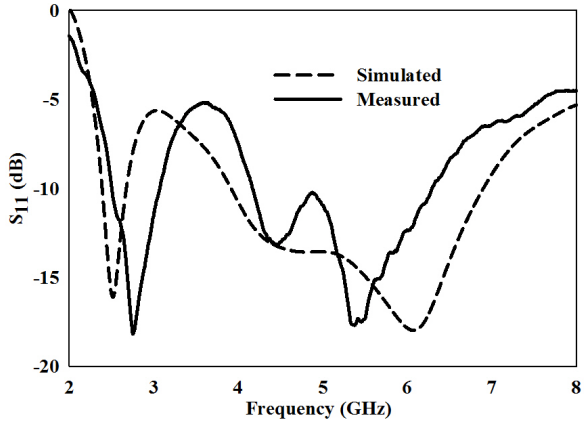

Figure 4. Simulated and measured S_{11} responses of the single antenna unit.

The simulated and measured S_{11} characteristics of the single antenna are depicted in Fig. 4. The measured -10 dB IBWs are 500 MHz (2.5 GHz to 3 GHz) and 2150 MHz (4.17 GHz to 6.32 GHz). Here, a good agreement between the simulated and measured responses is observed.

3. INTEGRATION OF QUAD-ELEMENT MIMO ANTENNA

By placing the antenna components in an orthogonal arrangement and spacing the two antennas by 10 mm, the unit antenna building block given in previous juncture is changed to form quad-element MIMO antenna. Fig. 5(a) shows the schematic geometry of the proposed MIMO antenna with length $L_1 = 60$ mm, and Figs. 5(b) and (c) portray photographs of the fabricated MIMO antenna.

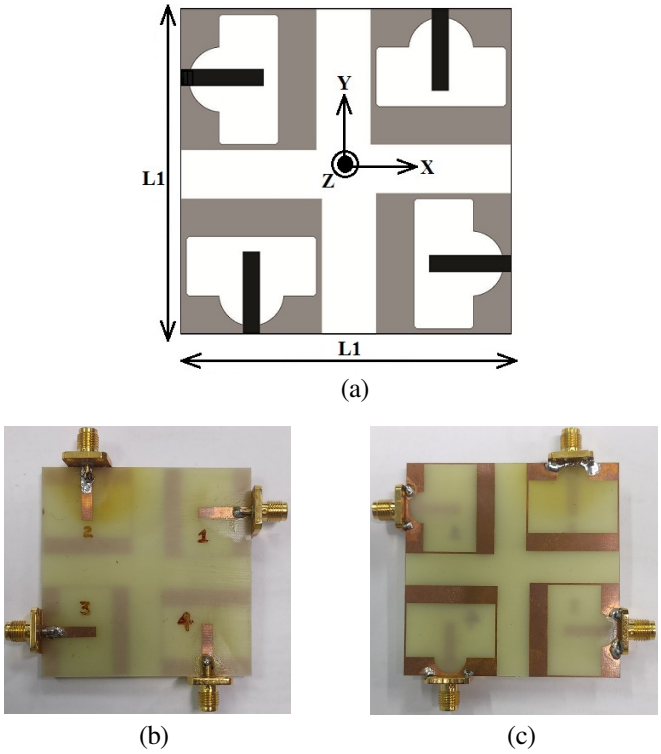

Figure 5. Schematic geometry of the contemplated four-element MIMO antenna. (a) Fabricated MIMO antenna-top view, (b) Fabricated MIMO antenna-bottom view.

3.1. Impedance Performance

Figure 6 shows the simulated S_{11} and measured S_{11}, S_{12}, S_{13}, and S_{14} values for the intended quad-element MIMO antenna. The measured value of S_{11} ranges from 2.42 to 3.07 (23.7%) for the first band and 4.14 to 6.37 (42.2%) for the second band. The minimum isolation of S_{12} is 25.62 dB at 5.3 GHz; S_{13} is 25.26 dB at 4.1 GHz; and S_{14} is 27.68 dB at 4.21 GHz.

3.2. Radiation Performance

The far-field measurements of the presented quad-element MIMO antenna are completed inside an anechoic chamber. The measured radiation patterns for elevation (E-plane) and azimuth (H-plane) planes for 2.4 GHz, 2.6 GHz, 5.2 GHz, and 5.8 GHz frequencies are shown in Figs. 7(a) to 7(d). Nearly omnidirectional radiation pattern is witnessed along the azimuth plane and excellent bidirectional radiation pattern along elevation plane at all the four frequencies. The gain performance of the proposed antenna is measured using the gain comparison method. The quad-element MIMO antenna delivers

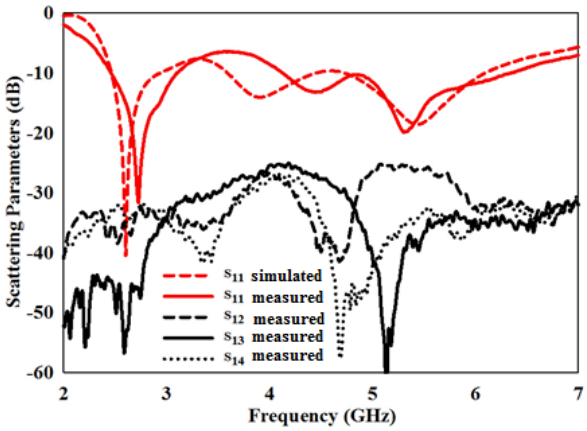

Figure 6. Simulated and measured scattering parameters of the 4 port MIMO antenna.

maximal gain of 2.8 dBi and 4.91 dBi at the first and second band, respectively. Also, the radiation efficiency performance of the quad-element MIMO antenna is measured using wheeler cap method. The proposed antenna provides a measured efficiency of 74% for the first band and 75% for the second band. Table 1 shows the measured IBW, minimum and maximum antenna isolation, measured gain, and measured radiation efficiency for the two operating bands.

Table 1. Measured parameters of the MIMO antenna.

Band (GHz)	2.42–3.07	4.14–6.37
Bandwidth (MHz)	650 (23.72%)	2320 (42.4%)
Maximum isolation (dB)	38	60
Minimum isolation (dB)	34	26
Measured gain (dBi)	2.8	4.91
Measured Radiation Efficiency (%)	74	75

3.3. Diversity Capabilities of Four-Element MIMO Antenna

The envelope correlation coefficient (ECC) of presented MIMO antenna is marked in Fig. 8. The ECC characterizes correlation among different single-antenna elements in a MIMO system. For an uncorrelated MIMO antenna system, the typical ECC value is zero. But for practical scenarios the satisfactory ECC values are below 0.05. Using scattering parameters [17], the ECC values can be calculated and depicted in Equation (1), where Rho_{ij} represents the ECC. Also, by using radiation pattern method [1], i.e., by employing Equation (2), ECC can be calculated. Here Equation (1) is used to calculate ECC values because it contains fewer variables than Equation (2). It is noted from Fig. 8 that the ECC values are below 0.05 for the two frequency ranges, signifying excellent MIMO antenna functioning.

$$Rho_{ij} = \frac{\left|S_{ii}^{*}S_{ij} + S_{ji}^{*}S_{jj}\right|^{2}}{\left(1-\left(|S_{ii}|^{2}+|S_{ji}|^{2}\right)\right)\left(1-\left(|S_{jj}|^{2}+|S_{ij}|^{2}\right)\right)} \tag{1}$$

$$Rho_{ij} = \frac{\left|\int_{\Omega}\left[XPR\cdot E_{\theta i}E_{\theta j}^{*}P_{\theta} + E_{\phi i}E_{\phi j}^{*}P_{\phi}\right]d\Omega\right|^{2}}{\int_{\Omega}\left\{XPR\cdot E_{\theta i}E_{\theta j}^{*}P_{\theta} + E_{\phi i}E_{\phi i}^{*}P_{\phi}\right\}d\Omega \times \int_{\Omega}\left\{XPR\cdot E_{\theta j}E_{\theta j}^{*}P_{\theta} + E_{\phi j}E_{\phi j}^{*}P_{\phi}\right\}d\Omega} \tag{2}$$

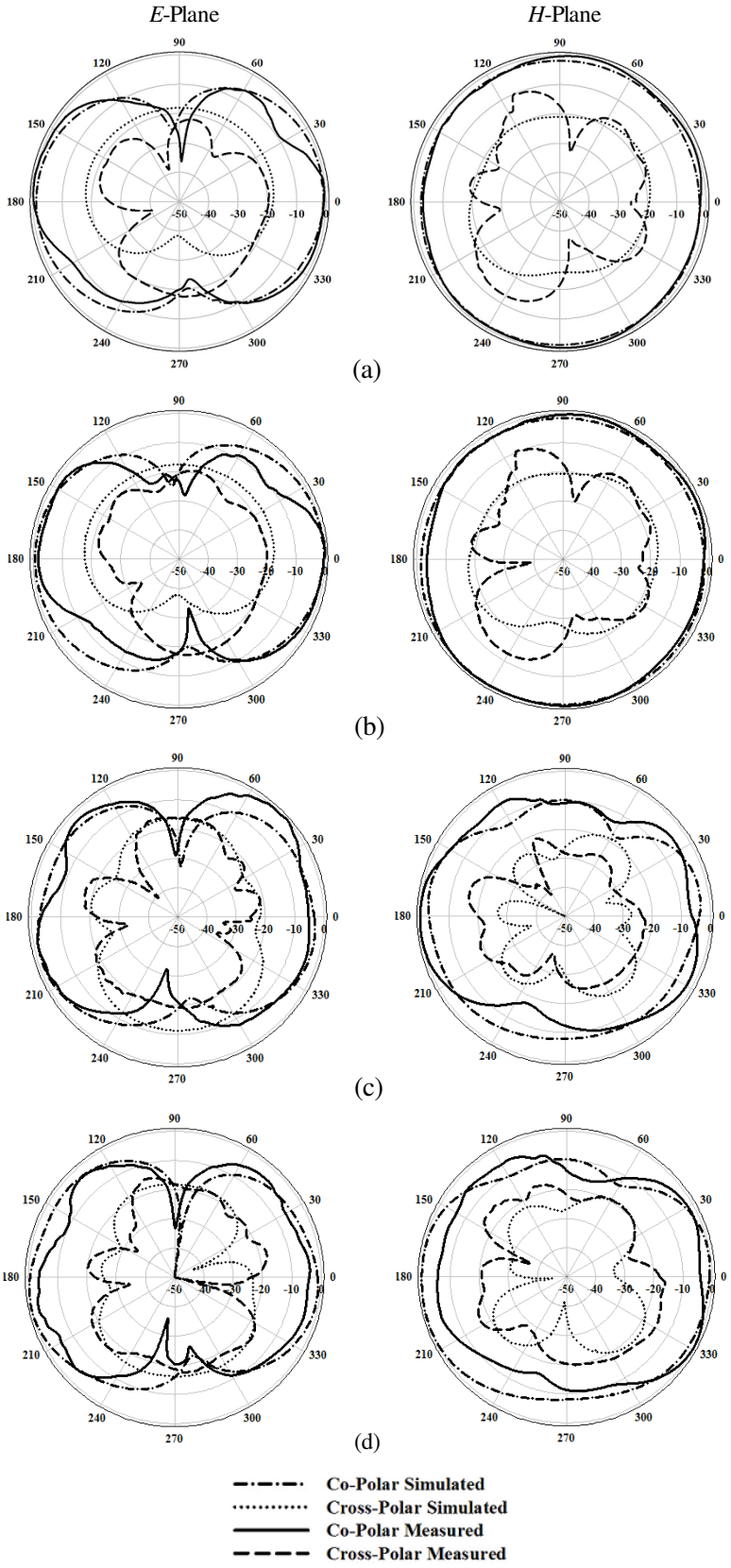

Figure 7. Measured and simulated two-dimensional radiation pattern. (a) 2.4 GHz, (b) 2.6 GHz, (c) 5.2 GHz and (d) 5.8 GHz.

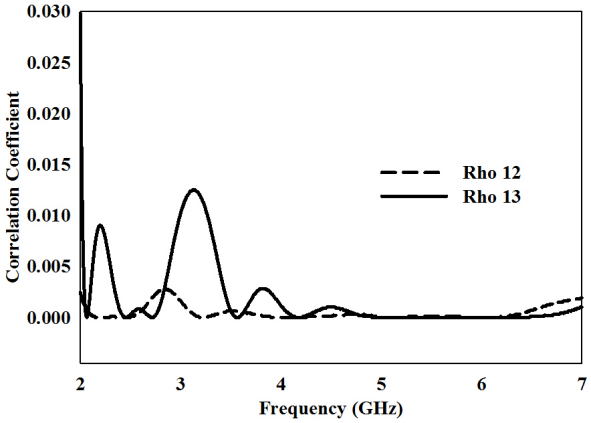

Figure 8. Envelope correlation coefficient between antenna 1 and 2 (Rho_{12}) and between antenna 1 and 3 (Rho_{13}).

Here XPR is the cross polarization ratio. P_θ and P_ϕ represent vertically and horizontally polarized incident wave's statistical power spectrum distributions.

Table 2 compares the accomplishment of the intended dual-band quad-element MIMO antenna with other MIMO antenna works in the literature. From Table 2, it is understood that the proposed antenna provides better antenna performance than existing antennas.

Table 2. Comparison of existing MIMO antennas with the proposed four-element MIMO antenna.

References	Total Antenna Size (mm^3)	No. of antenna elements	No. of Bands	Frequency (GHz)	IBW (%)	Isolation (dB)
[2]	$70 \times 70 \times 1.52$	4	2	2.58	14.3	21
				5.3	12.8	21
[3]	$60 \times 80 \times 1.6$	4	1	2.45	4.08	25
[6]	$62 \times 62 \times 0.8$	8	2	2.45	8.5	≈ 18
				5.5	14.5	≈ 15
[7]	$120 \times 140 \times 1.6$	4	1	2.4	45.83	15
[8]	$100 \times 50 \times 0.8$	2	2	2.45	16.2	≈ 20
				5.8	3.21	≈ 20
[9]	$50 \times 100 \times 0.8$	4	2	2.45	10.1	≈ 20
				5.2	3.85	≈ 30
[10]	$54 \times 54 \times 1.57$	4	1	10	3.4	23.78
[11]	$30 \times 40 \times 1.6$	4	1	4.5	58.56	17.5
[13]	$66 \times 66 \times 1.6$	4	1	2.5	16	17
[15]	$100 \times 100 \times 12.6$	2	1	2.45	9.15	6.8
[16]	$105 \times 72 \times 10$	2	1	2.6	< 4	10
[17]	$180 \times 90 \times 27$	2	2	2.75	25	27
				5.45	12	25
Proposed Antenna	$\mathbf{60 \times 60 \times 1.6}$	**4**	**2**	**2.74**	**23.7**	**34**
				5.25	**42.4**	**26**

4. CONCLUSION

A four-port MIMO antenna with a self-decoupling mechanism, introduced for improved isolation is explained in this work. A rectangular and semicircular slot in the ground plane forming the defective ground structure is capable of providing wider impedance bandwidth and enhanced isolation between the elements for the two frequency bands. The overall dimension of intended MIMO antenna is 60 mm $\times$ 60 mm $\times$ 1.6 mm because of defective ground structure. For frequency ranges pivoted on 2.47 GHz and 5.25 GHz, the planned quad-element antenna has wider impedance bandwidth of 23.7% and 42.4%, respectively, and a minimum isolation of 34 dB and 26 dB. Furthermore, the antenna's good radiation patterns, moderate gain, low correlation coefficient, and acceptable radiation efficiency suggest that it will be suitable for sub-6 GHz 5G applications.

ACKNOWLEDGMENT

Authors gratefully acknowledge the support from University grants commission through research fellowship and CSIR through Emeritus Scientist Scheme.

REFERENCES

1. Anitha, R., P. V. Vinesh, K. C. Prakash, P. Mohanan, and K. Vasudevan, "A compact quad element slotted ground wideband antenna for MIMO applications," *IEEE Trans. Antennas Propag.*, Vol. 64, No. 10, 4550–4553, 2016.
2. Malviya, L., R. K. Panigrahi, and M. V. Kartikeyan, "A 2 $\times$ 2 dual-band MIMO antenna with polarization diversity for wireless applications," *Progress In Electromagnetics Research C*, Vol. 61, 91–103, 2016.
3. Li, H., J. Xiong, and S. He, "A compact planar MIMO antenna system of four elements with similar radiation characteristics and isolation structure," *IEEE Antennas Wireless Propag. Lett.*, Vol. 8, 1107–1110, 2009.
4. Ding, Y., Z. Du, K. Gong, and Z. A. Feng, "Four-element antenna system for mobile phones," *IEEE Antennas Wireless Propag. Lett.*, Vol. 6, 655–658, 2007.
5. Zhang, S., P. Zetterberg, and S. He, "Printed MIMO antenna system of four closely-spaced elements with large bandwidth and high isolation," *Electronics Lett.*, Vol. 46, No. 15, 1052–1053, 2010.
6. Liu, Y. Y., Z. H. Tu, and Q. X. Chu, "Differentially T-shape slot antenna with high common-mode suppression for 2.4/5.2/5.8 GHz WLAN MIMO systems," *Asia-Pacific Microwave Conference*, 1–3, Nanjing, 2015, doi: 10.1109/APMC.2015.7411767.
7. Kordalivand, A. M., T. A. Rahman, and M. Khalily, "Common elements wideband MIMO antenna system for Wi-Fi/LTE access-point applications," *IEEE Antennas Wireless Propag. Lett.*, Vol. 13, 1601–1604, 2014.
8. Singh, H. S., G. K. Pandey, P. K. Bharti, and M. K. Meshram, "A compact dual-band diversity antenna for WLAN applicationswith high isolation," *Microw. Optical Technol. Lett.*, Vol. 57, 906–912, 2015.
9. Lee, J. N., K. C. Lee, N. Park, and J. Park, "Design of dual-band MIMO antenna with high isolation for WLAN mobile terminal," *ETRI Journal*, Vol. 35, 177–187, 2013.
10. Khandelwal, M. K., "Metamaterial based circularly polarized four-port MIMO diversity antenna embedded with slow-wave structure for miniaturization and suppression of mutual coupling," *AEU — Int. J. Electron. Commun.*, Vol. 121, 153241, 2020.
11. Kulkarni, J., A. Desai, and C. Y. D. Sim, "Wideband four-port MIMO antenna array with high isolation for future wireless systems," *AEU — Int. J. Electron. Commun.*, Vol. 128, 153507, 2021.
12. Ameen, M., O. Ahmad, and R. K. Chaudhary, "Single split-ring resonator loaded self-decoupled dual-polarized MIMO antenna for mid-band 5G and C-band applications," *AEU — Int. J. Electron. Commun.*, Vol. 124, 153336, 2020.

13. Yussuf, A. A. and S. Paker, "Design of a compact quad-radiating element MIMO antenna for LTE/Wi-Fi application," *AEU — Int. J. Electron. Commun.*, Vol. 111, 152893, 2019.
14. Prabhu, P. and S. Malarvizhi, "Novel double-side EBG based mutual coupling reduction for compact quad port UWB MIMO antenna," *AEU — Int. J. Electron. Commun.*, Vol. 109, 146–156, 2019.
15. Imbert, M., P. J. Ferrer, and J. M. Gonzalez-Arbesu, "Assessment of the performance of a metamaterial spacer in a closely spaced multiple-antenna system," *IEEE Antennas Wireless Propag. Lett.*, Vol. 11, 720–723, 2012.
16. Panda, P. K. and D. Ghosh, "Isolation and gain enhancement of patch antennas using EMNZ superstrate," *AEU — Int. J. Electron. Commun.*, Vol. 86, 164–170, 2018.
17. Rezvani, M. and Y. Zehforoosh, "A dual-band multiple-input multiple-output microstrip antenna with metamaterial structure for LTE and WLAN applications," *AEU — Int. J. Electron. Commun.*, Vol. 93, 277–282, 2018.
18. Ibrahim, A. A. and M. A. Abdalla, "CRLH MIMO antenna with reversal configuration," *AEU — Int. J. Electron. Commun.*, Vol. 70, No. 9, 1134–1141, 2016.